Electroluminescence and multiphoton effects in a resonator driven by a tunnel junction

Jinshuang Jin,[1,2,3] Michael Marthaler,[3] and Gerd Schön[1,3,4]

[1]*Institute of Nanotechnology, Karlsruhe Institute of Technology (KIT), D-76021 Karlsruhe, Germany*

[2]*Department of Physics, Hangzhou Normal University, Hangzhou 310036, China*

[3]*Institut für Theoretische Festkörperphysik, Karlsruhe Institute of Technology (KIT), D-76131 Karlsruhe, Germany*

[4]*DFG Center for Functional Nanostructures, Karlsruhe Institute of Technology (KIT), D-76131 Karlsruhe, Germany*

(Received 30 July 2014; revised manuscript received 11 January 2015; published 23 February 2015)

We study a transmission line resonator which is driven by electrons tunneling through a voltage-biased tunnel junction. Using the Born-Markovian quantum master equation in the polaron basis we investigate the nonequilibrium photon state and emission spectrum of the resonator as well as properties of the transport current across the tunnel junction and its noise spectrum. The electroluminescence is optimized, with maximum peak height and narrow linewidth, when the back-action of the tunnel junction on the resonator and the damping of the resonator are similar in strength. For strong coupling between the resonator and tunnel junction, multiphoton effects create signatures in the transport current and current noise spectrum.

DOI: 10.1103/PhysRevB.91.085421 PACS number(s): 85.60.−q, 73.23.−b, 73.63.Rt, 72.70.+m

I. INTRODUCTION

Circuit quantum electrondynamics (cQED) of on-chip solid-state systems coupled to a microwave resonator has attracted much attention. The investigations were stimulated by the possibility of strong coupling between a superconducting qubit and a transmission line resonator [1–3].

This allowed demonstrating phenomena known from quantum optics in solid-state systems with unprecedented quality. Some examples are vacuum Rabi splitting [2,3], advanced applications of quantum state engineering [4–6], as well as single-qubit lasing and cooling [7–9].

The development of cQED is not restricted to superconducting systems but has also been extended to solid-state devices composed of gate-defined semiconductor quantum dots or multidot systems coupled to electromagnetic resonators [10–18]. Of particular interest is the interplay of electron transport through the dots and the excitation of photons in the resonator. Single-electron tunneling through a double-dot setup can produce a population inversion and induce a lasing state in the resonator, accompanied by pronounced features such as super- or sub-Poissonian noise of the transport current [13–15]. For a simpler system, a resonator driven by electrons tunneling through a single quantum dot, the nonequilibrium photon population has also been investigated [16,17].

Continuing to even more basic systems, the question arises: What is the nonequilibrium photon state created in the resonator by electrons tunneling across a single junction without intermediate quantum dots? Recently, such systems have been investigated experimentally, with the observation that the resonator influences the finite-frequency shot noise of the transport current through the junction similar to a thermal electromagnetic environment [19]. A comprehensive study of nonequilibrium effects in the resonator which is strongly coupled to a biased tunnel junction has not yet been performed, although the setup may find various applications. For instance, the system has been used as an effective charge detector for single-shot read-out of quantum-dot-based qubits [20–23], and as a displacement detector which can resolve the momentum and position of nanomechanical resonators with high precision [24–29]. Furthermore, it has been proposed that a tunnel junction can be used to generate squeezed light and microwave photon pairs [30,31].

In the present work we study the nonequilibrium photon state in a transmission line resonator which is strongly coupled to the electrons tunneling through a tunnel junction (TJ). We focus on the electroluminescence of the excited photons in the driven resonator, as well as the transport current through the tunnel junction and its noise spectrum.

In Sec. II, we introduce the model of the TJ-resonator circuit and present the quantum master equation describing the dynamics of the coupled system. We investigate the system in Sec. III for moderately strong coupling, where single-photon processes dominate the dynamics. In this limit we find analytic results. We then study numerically in Sec. IV multiphoton effects which get visible in what is called the ultrastrong coupling limit. We conclude with a summary.

II. METHODOLOGY

A. The system

We consider a superconducting transmission line resonator strongly coupled to a tunnel junction in a setup as sketched in Fig. 1. The corresponding Hamiltonian is given by ($\hbar = 1$),

$$H_{\rm tot} = \sum_{\alpha k} \varepsilon_{\alpha k} c^\dagger_{\alpha k} c_{\alpha k} + \sum_{kk'} (t_{kk'} c^\dagger_{Lk} c_{Rk'} + \text{H.c.}) + \omega_r a^\dagger a + g \sum_k (c^\dagger_{Rk} c_{Rk} - c^\dagger_{Lk} c_{Lk})(a + a^\dagger). \quad (1)$$

It describes the tunnel junction between the left and right ($\alpha = L, R$) reservoirs with single-particle energies $\varepsilon_{\alpha k}$ and tunneling amplitudes $t_{kk'}$ between the two reservoirs.

The resonator is modeled by a harmonic oscillator with frequency ω_r. The coupling of the two subsystems with strength g is assumed to be induced by the electric field of the resonator across the tunnel junction, as illustrated in Fig. 1, which shifts the chemical potentials of the two reservoirs. Here we assume shifts of equal magnitude for both sides, but the generalization is straightforward.

We proceed using the polaron transformation, $\widetilde{H} = UHU^\dagger$ with $U = \exp[\frac{g}{\omega_r} \sum_k (c^\dagger_{Rk} c_{Rk} - c^\dagger_{Lk} c_{Lk})(a^\dagger - a)]$. It

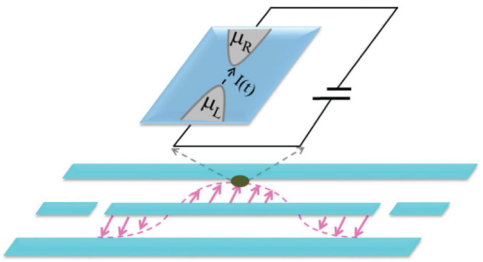

FIG. 1. (Color online) Schematic view of a tunnel junction-resonator circuit. The junction is placed at a maximum of the electric field of the transmission line resonator in order to maximize the dipole interaction.

transforms the Hamiltonian (1) to

$$\widetilde{H}_{\rm tot} = \sum_{\alpha k} \varepsilon_{\alpha k} c^\dagger_{\alpha k} c_{\alpha k} + \omega_r a^\dagger a + \sum_{kk'} (t_{kk'} c^\dagger_{Lk} c_{Rk'} e^{-\lambda(a^\dagger - a)} + \text{H.c.}). \quad (2)$$

Here we neglected a trivial energy shift in the electrodes and introduced the dimensionless coupling strength $\lambda \equiv 2g/\omega_r$. The coupling of the transmission-line resonator to its reservoir is also slightly affected by this transformation, and we discuss this effect in the appendix. In the interaction picture with respect to the electronic reservoirs $H_{\rm B} = \sum_{\alpha k} \varepsilon_{\alpha k} c^\dagger_{\alpha k} c_{\alpha k}$, we recast the Hamiltonian (2) as $\widetilde{H}_{\rm tot}(t) = H_r + H'(t)$ with $H_r = \omega_r a^\dagger a$ and coupling

$$H'(t) = F^\dagger(t) Q + Q^\dagger F(t). \quad (3)$$

The operators $F^\dagger(t) = \sum_{kk'} t_{kk'} c^\dagger_{Lk} c_{Rk'} e^{i\Delta_{kk'}t}$ with $\Delta_{kk'} = \varepsilon_{Lk} - \varepsilon_{Rk'}$ and $Q = \exp[-\lambda(a^\dagger - a)]$ refer to the tunnel junction and resonator, respectively. For later use we introduce the correlation functions of the bath accounting for forward (L to R) and backward tunneling, $C^{(+)}(t) \equiv \langle F^\dagger(t) F(0)\rangle_{\rm B}$ and $C^{(-)}(t) \equiv \langle F(t) F^\dagger(0)\rangle_{\rm B}$, respectively. Here $\langle ... \rangle_{\rm B}$ stands for the statistical average over both electron reservoirs. They are assumed to be in thermal equilibrium, which implies that the correlators reduce to

$$C^{(\pm)}(t) = \sum_{kk'} e^{\pm i \Delta_{kk'} t} |t_{kk'}|^2 f^\pm_{Lk} f^\mp_{Rk'}. \quad (4)$$

Here we introduced the Fermi-Dirac function of the α lead $f^+_{\alpha k} \equiv f_{\alpha k} = [e^{\beta(\varepsilon_{\alpha k} - \mu_\alpha)} + 1]^{-1}$ with $\beta = 1/(k_B T)$ and $f^-_{\alpha k} = 1 - f_{\alpha k}$. We focus on the limit of a tunnel junction with tunneling probabilities of each channel much smaller than unity, and we assume momentum-independent tunneling amplitudes, $t_{kk'} = t$. Combined with the densities of states ν_α of the α reservoir they determine the tunneling resistance R and dimensionless tunneling strength $\eta = 1/(2e^2 R) = \pi |t|^2 \nu_L \nu_R$. We assume $\eta \ll 1$ to be small. The bath correlators in Fourier space, $\widetilde{C}^{(\pm)}(\omega) = \int_{-\infty}^{\infty} dt\, e^{i\omega t} C^{(\pm)}(t)$, thus become

$$\widetilde{C}^{(\pm)}(\omega) = \frac{2\eta(\omega \pm \text{eV})}{1 - e^{-\beta(\omega \pm \text{eV})}}. \quad (5)$$

They account for forward and backward tunneling processes with energy absorption ($\omega > 0$) and emission ($\omega < 0$). Here $\text{eV} = \mu_L - \mu_R$ is the applied bias voltage across the tunnel junction.

B. Quantum master equation

Starting from the total density operator $\rho_{\rm tot}(t)$ of the combined TJ-resonator system one obtains the reduced density matrix of the resonator by tracing out the bath degrees of freedom of the two electronic reservoirs, $\rho(t) = {\rm tr}_B[\rho_{\rm tot}(t)]$. Treating $H'(t)$ as perturbation and expanding up to second order leads to the Born-Markovian master equation,

$$\dot\rho(t) = -i[H_r, \rho(t)] + \mathcal{L}_\kappa \rho(t) + \mathcal{L}_B \rho(t) \equiv \mathcal{L}\rho(t). \quad (6)$$

The first term describes the coherent evolution, while the second term is the standard decay term of the resonator with decay rate κ, and the third accounts for the effect of the tunnel junction. They are given by

$$\mathcal{L}_\kappa \rho = \kappa(n_{\rm th}+1)\big[a\rho a^\dagger - \tfrac{1}{2}(a^\dagger a\rho + \rho a^\dagger a)\big] + \kappa n_{\rm th}\big[a^\dagger \rho a - \tfrac{1}{2}(aa^\dagger \rho + \rho aa^\dagger)\big], \quad (7a)$$

$$\mathcal{L}_B \rho = \tfrac{1}{2}(\widetilde{Q}_- \rho Q^\dagger + Q\rho \widetilde{Q}_-^\dagger - Q^\dagger \widetilde{Q}_- \rho - \rho \widetilde{Q}_-^\dagger Q + \widetilde{Q}_+^\dagger \rho Q + Q^\dagger \rho \widetilde{Q}_+ - Q\widetilde{Q}_+^\dagger \rho - \rho \widetilde{Q}_+ Q^\dagger). \quad (7b)$$

Here $n_{\rm th} = [\exp(\beta\omega_r) - 1]^{-1}$ is the thermal photon number in the resonator, and we introduced the operators,

$$\widetilde{Q}_\pm = \int_{-\infty}^{\infty} dt\, C^{(\pm)}(t) e^{\pm i H_r t} Q e^{\mp i H_r t}.$$

The further calculations are done in the basis of Fock states, $H_r|n\rangle = n\omega_r|n\rangle$, of the photons in the resonator, for which the operator entering the coupling Eq. (3) is expressed as $Q = \sum_{nm} Q_{mn} |m\rangle\langle n|$, with $Q_{mn} = \langle m|e^{-\lambda(a^\dagger - a)}|n\rangle$. Correspondingly, the elements of the operator $\widetilde{Q}_\pm$ are calculated via $\langle m|\widetilde{Q}_\pm|n\rangle = \widetilde{C}^{(\pm)}(\pm\omega_{mn}) Q_{mn}$, with $\omega_{mn} \equiv (m-n)\omega_r$ and $\widetilde{C}^{(\pm)}(\pm\omega_{mn})$ given by Eq. (5).

To proceed, we truncate the Hilbert space of the resonator to a finite number N of photon number states. The numerical evaluation is performed by recasting Eq. (6) in vector form [32], $\dot{\vec\rho} = G\vec\rho$. The reduced $N \times N$ density matrix ρ is arranged as an N^2-dimensional vector $\vec\rho$, and G is a $N^2 \times N^2$ superoperator acting on the Liouvillian space of the system.

Based on the master equation in the stationary limit, the emission spectrum of the resonator,

$$S_{\rm r}(\omega) \equiv \lim_{t\to\infty} \int_{-\infty}^{\infty} d\tau \langle a^\dagger(t) a(t+\tau)\rangle e^{i\omega\tau}, \quad (8)$$

as well as the second-order correlation function $g^{(2)}(\tau) = \lim_{t\to\infty} \langle a^\dagger(t) a^\dagger(t+\tau) a(t+\tau) a(t)\rangle / \langle a^\dagger(t) a(t)\rangle^2$ can be calculated via the quantum regression theorem [33]. Starting from $I(t) = -e\, d\langle n_R(t)\rangle/dt$ with $n_R = \sum_k c^\dagger_{Rk} c_{Rk}$ we obtain the transport current [34] $I(t) = \langle \hat I(t)\rangle = {\rm Tr}[\hat I \rho(t)]$ with current operators,

$$\hat I \rho(t) = \frac{e}{2}[Q^\dagger \rho(t) \widetilde{Q}_+ - \widetilde{Q}_- \rho(t) Q^\dagger + \text{H.c.}]. \quad (9)$$

From this we calculate the average current $I(t)$ and the current noise spectrum,

$$S_I(\omega) = \int_{-\infty}^{\infty} dt\, \langle\{\delta\hat{I}(t),\delta\hat{I}(0)\}\rangle e^{i\omega t}, \tag{10}$$

with $\delta\hat{I}(t) = \hat{I}(t) - I$. Here we consider the symmetrized correlation function since it is real and corresponds most directly to what is measured by a classical detector [35]. Also the noise spectrum can be calculated using the quantum regression theorem [15].

In the present work we concentrate on the sequential-tunneling regime of single-electron processes, valid in the limit $\eta \ll 1$. We assume that the resonator has a high Q factor. Specifically we will present results for $Q = 2\times10^4$, corresponding to a decay rate $\kappa = 5\times10^{-5}\omega_r$. It is much smaller than both the tunneling rate and coupling strength, $\kappa/\omega_r \ll \eta,\lambda$. Under these conditions the Born-Markov approximation is valid for stationary quantities for nonzero temperatures at all voltages, which allows us to study stationary quantities like the current for all voltages, eV $\neq 0$. For the calculation of dynamic quantities, like the spectral functions of the current and the photon emission, the Born-Markov approximation is sufficient as long as the frequencies satisfy $\omega \leqslant$ eV. Since we will concentrate on the regime where a substantial number of photons are created, we will operate in the limit of moderately large voltages and the Born-Markov approximation is well justified.

III. MODERATE COUPLING STRENGTH

For weak to moderate coupling strength, $\lambda \ll 1$ (but still $\kappa/\omega_r \ll \lambda$), we proceed in an expansion up to second order, i.e., $Q = e^{-\lambda(a^\dagger - a)} \approx 1 - \lambda(a^\dagger - a) + \frac{1}{2}\lambda^2(a^\dagger - a)^2$. We assume low temperatures, where the electrons tunnel only from the left to the right lead without the reverse process [i.e., $\widetilde{C}^{(-)}(\omega) = 0$], and the number of thermal photons in the resonator vanishes, $n_{\rm th} = 0$. In this case the master equation for the oscillator reduces to

$$\dot{\rho} = -i[H_r,\rho(t)] + (\kappa+\Gamma_+)\left[a\rho a^\dagger - \tfrac{1}{2}(a^\dagger a\rho + \rho a^\dagger a)\right] + \Gamma_-\left[a^\dagger\rho a - \tfrac{1}{2}(aa^\dagger\rho + \rho aa^\dagger)\right], \tag{11}$$

with rates $\Gamma_\pm = \lambda^2\widetilde{C}^{(+)}(\pm\omega_r)$. In the considered limit we could make use of the rotating wave approximation. The resulting master equation (11) accounts for single-photon processes, i.e., processes where electrons tunneling through the junction are associated with the emission or absorption of a single photon in the resonator with rates Γ_- and Γ_+, respectively. Interestingly, the second-order term of the expansion of Q does not enter the master equation, however, it does modify the average current to be studied later.

From Eq. (11) we see that the resonator is subject to an effective decay rate [36],

$$\kappa_{\rm eff} = \Gamma_+ - \Gamma_- + \kappa \approx 4\eta\lambda^2\omega_r + \kappa\,, \tag{12}$$

and the average photon number is

$$\bar{n} = \frac{\Gamma_-}{\Gamma_+ - \Gamma_- + \kappa} \approx \frac{\eta\lambda^2(eV-\omega_r)}{2\eta\lambda^2\omega_r + \kappa/2}\Theta(\text{eV}-\omega_r)\,. \tag{13}$$

Here, Θ is the step function, $\bar{n} = \langle a^\dagger a\rangle = \sum_n nP_n$ with $P_n = \rho_{nn}$. The corresponding photon distribution, $P_n \approx \langle n\rangle^n/(1+\langle n\rangle)^{n+1}$ reduces to a Bose-Einstein distribution with effective temperature,

$$k_BT_{\rm eff} \approx \omega_r/\ln\left[\frac{\eta\lambda^2(\text{eV}+\omega_r)+\kappa/2}{\eta\lambda^2(\text{eV}-\omega_r)}\right]\Theta(\text{eV}-\omega_r), \tag{14}$$

which coincides with the intensity distribution of classical chaotic light [37,38]. A similar result has been derived for a resonator driven by electrons tunneling through a single quantum dot [16]. The effective temperature has also been obtained in previous work [26–29] on quantum point contacts coupled to a mechanical oscillator in the limit eV $\gg \omega_r$. If λ is sufficiently small to neglect higher order resonances and $4\eta\lambda^2\omega_r \gg \kappa$, we recover the result $k_BT_{\rm eff} \approx$ eV/2 obtained previously.

For the second-order correlation function we get

$$g^{(2)}(\tau) = 1 + e^{-\kappa_{\rm eff}\tau}. \tag{15}$$

It displays bunching, $g^{(2)}(0) = 2$, for vanishing time delay and approaches $g^{(2)}(\tau\to\infty) = 1$ in the opposite limit when no correlations exist between the excited photons.

From the master equation we can determine the emission spectrum of the resonator, with the result,

$$S_{\rm r}(\omega) = \frac{\kappa_{\rm eff}\bar{n}}{(\omega_r-\omega)^2 + (\kappa_{\rm eff}/2)^2}. \tag{16}$$

It has a maximum height at $\omega = \omega_r$,

$$S_{\rm r}(\omega_r) = \frac{4\bar{n}}{\kappa_{\rm eff}} \approx \frac{2\eta\lambda^2(\text{eV}-\omega_r)}{(2\eta\lambda^2\omega_r+\kappa/2)^2}\Theta(\text{eV}-\omega_r). \tag{17}$$

Interestingly, with increasing coupling strength λ or tunneling strength η, the height of the peak first increases and then decreases with simultaneous broadening of the linewidth as shown in Fig. 2. This nonmonotonic behavior arises because the electron tunneling through the junction not only excites photons in the resonator but simultaneously introduces dissipation, as described by the contribution $4\eta\lambda^2\omega_r$ to the decay rate Eq. (12). From Eq. (17) we find that the emission is strongest when the parameters satisfy the relation,

$$\eta_{\rm p}\lambda_{\rm p}^2 = \frac{\kappa}{4\omega_r}, \tag{18}$$

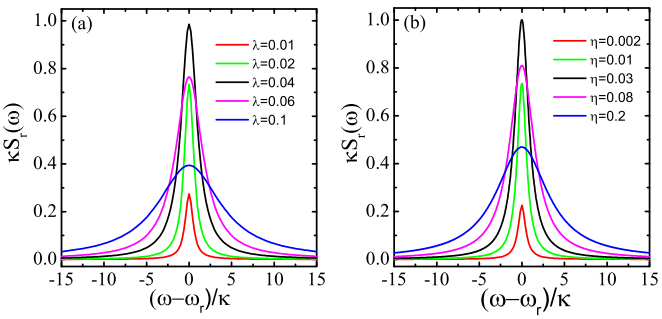

FIG. 2. (Color online) The emission spectrum of the resonator $S_r(\omega)$ near the one-photon resonance, (a) for $\eta = 0.01$ and different coupling strengths λ, and (b) for $\lambda = 0.02$ and different tunneling rates η. The other parameters are as follows: low temperature $k_BT = 0.02\omega_r$ and bias voltage eV $= 3\omega_r$.

leading to $S_r^{\max}(\omega_r) = (\mathrm{eV} - \omega_r)\Theta(\mathrm{eV} - \omega_r)/(2\kappa\omega_r)$, while the linewidth is still narrow, $(\kappa_{\mathrm{eff}})_p/2 = \kappa$.

This means that the electroluminescence is optimized when the dissipation induced by the tunnel junction, $4\eta\lambda^2\omega_r$, is similar in strength to the decay rate κ of the resonator.

In the considered limit (i.e., up to order λ^2) we get from Eq. (9) and Eq. (10) the average current,

$$I = (1-\lambda^2)\widetilde{C}^{(+)}(0) + \lambda^2\widetilde{C}^{(+)}(-\omega_r) \approx 2\eta(1-\lambda^2)\mathrm{eV} + 2\eta\lambda^2(\mathrm{eV}-\omega_r)\Theta(\mathrm{eV}-\omega_r). \quad (19)$$

Below the onset of single-photon processes the transport current is suppressed by the coupling to the resonator. This effect is described by the Franck-Condon factor $(1-\lambda^2/2)^2$ renormalizing the tunneling rate [16]. Above the threshold, when photons can be exited, the current grows as described by the second term.

The properties of the current noise at $\omega = \omega_r$ are dominated by single-photon processes, which are described by the linear term in the coupling Hamiltonian Eq. (3), $Q \propto 1 - \lambda(a^\dagger - a)$. Proceeding in this first-order approximation we find that the current noise at $\omega = \omega_r$ is proportional to the difference between the rate for tunneling with photon emission $\widetilde{C}^{(\pm)}(-\omega_r)$ and the one with photon absorption $\widetilde{C}^{(\pm)}(\omega_r)$,

$$S_I(\omega) \approx 2eI + \sum_{+,-} \frac{c_1\kappa_{\mathrm{eff}}/2}{(\omega \pm \omega_r)^2 + (\kappa_{\mathrm{eff}}/2)^2}\Theta(\mathrm{eV}-\omega_r), \quad (20)$$

with

$$c_1 = 4e\eta\lambda^2 \sum_{\pm}[\widetilde{C}^{(\pm)}(-\omega_r) - \widetilde{C}^{(\pm)}(\omega_r)] \quad (21)$$

$$= -8e\eta^2\lambda^2\omega_r[\mathrm{eV} + (\bar{n} - 1/2)\omega_r]. \quad (22)$$

The result is displayed in Fig. 3. The combination of electrons tunneling through the junction with the emission and absorption of photons in the resonator leads to a dip in the spectrum at $\omega = \pm\omega_r$. The dip gets deeper, i.e., $|S(\omega_r) - 2eI| \approx 2|c_1|/\kappa_{\mathrm{eff}}$ increases, with growing coupling or tunneling strengths. The linewidth κ_{eff} of the current noise dip is the same as linewidth of the emission spectrum of the resonator. A comparison with the numerical solution of the full problem, presented in the following section, shows that analytic results obtained so far are valid for weak to moderate coupling strength as long as $\lambda \lesssim 0.2$.

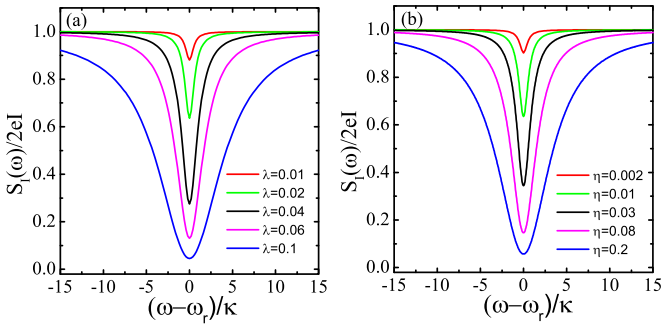

FIG. 3. (Color online) The noise spectrum of the transport current through the junction $S_I(\omega)$, (a) for $\eta = 0.01$ and different coupling strengths λ, and (b) for $\lambda = 0.02$ and different tunneling rates η. The parameters are the same as in Fig. 2.

IV. ULTRASTRONG COUPLING

We turn now to the so-called ultrastrong-coupling regime where the coupling strength between tunnel junction and resonator is of the same order as the resonator frequency. Specifically we consider $0.2 < \lambda = 2g/\omega_r \lesssim 2$. Although more difficult to realize in an experiment, these values are still realistic, and this limit displays interesting new properties.

In the strong coupling regime the expansion up to order λ^2 analyzed in Sec. III is no longer sufficient. Instead processes associated with the excitation of multiple photons, which follow from expanding $Q = e^{-\lambda(a^\dagger - a)}$ to higher orders in λ, gain importance. In order to study these processes we solved the equations introduced above numerically without further approximations. In contrast to the single-photon limit, the average photon number, shown in Fig. 4, in general depends nonlinearly on the bias voltage and even decreases with increasing coupling strength.

The photon state differs from a thermal state; e.g., as shown in the inset of Fig. 4(b), the second-order correlation function deviates from the value $g^{(2)}_{\mathrm{thermal}}(0) = 2$, which would be found for a thermal (chaotic) state.

The effect of the multiphoton processes on the transport current manifests itself in a nonlinear dependence on the bias voltage as shown in Fig. 5(a). Simultaneously, the multiphoton effects enhance the current fluctuations and induce the super-Poissonian behavior in the zero-frequency shot noise, as shown in Fig. 6(a). The multiphoton effects can also be observed in the current noise spectrum. In an expansion up to fourth order in the coupling we obtain the noise spectrum near $\omega = 0$ and $\omega = \pm 2\omega_r$,

$$S_I(\omega) \propto e\eta^2\lambda^4\left[\frac{c_0\kappa_{\mathrm{eff}}}{\omega^2 + \kappa_{\mathrm{eff}}^2} + \sum_{+,-}\frac{c_2\kappa_{\mathrm{eff}}}{(\omega \pm 2\omega_r)^2 + \kappa_{\mathrm{eff}}^2}\right],$$

with positive coefficients $c_0 > 0$ and $c_2 > 0$. The two-photon processes lead to peaks in the noise spectrum at $\omega = 0$ and

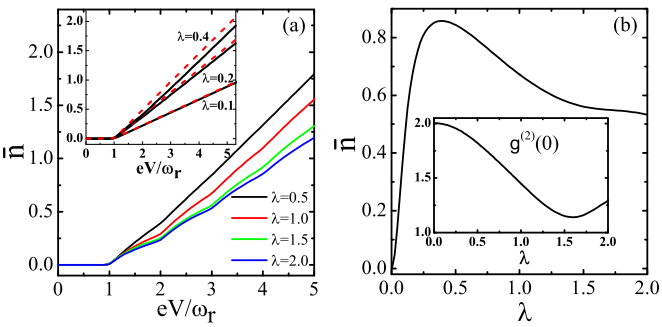

FIG. 4. (Color online) The average number of photons excited in the resonator (a) as a function of the bias voltage eV for different coupling strengths λ, and (b) as a function of the coupling strength λ for $\mathrm{eV} = 3\omega_r$. The other parameters are as follows: low temperature $k_BT = 0.02\omega_r$ and tunneling rate $\eta = 0.001$. In the inset in (a) we compare results for moderate coupling strength based on the numerical calculation (solid line) and analytical expression of Eq. (13) (dashed line).

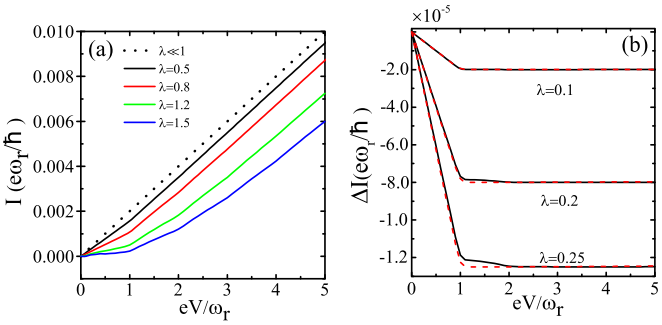

FIG. 5. (Color online) (a) The average tunneling current through the junction versus bias voltage for different coupling strength. With increasing λ multiphoton effect becomes more significant. (b) For better resolution the lowest order tunneling current is subtracted, i.e., $\Delta I = I - 2\eta \mathrm{eV}$. For moderate coupling strength we compare the numerical results based on the exact Eq. (9) (solid line) and approximate expressions of Eq. (19) (dashed line). The other parameters are the same as in Fig. 4.

$\omega = \pm 2\omega_r$ with linewidth determined by κ_{eff}, as shown in Figs. 6(a) and 6(c). The feature at zero frequency corresponds to single-electron tunneling processes accompanied by a virtual emission and absorption of a photon, while the feature at $\omega = \pm 2\omega_r$ comes from single-electron tunneling processes which are accompanied by emission (absorption) of two photons.

Approximately, we find $c_0 \propto \sum_{+,-}[2C^{(+)}(\pm\omega_r) - C^{(+)}(0)]^2 > 0$ and $c_2 \propto \sum_{+,-}[2C^{(+)}(\pm\omega_r) - C^{(+)}(\pm 2\omega_r)]^2 > 0$.

Compared to the features at $\omega = \pm\omega_r$, the noise spectra at $\omega = 0$ and $\omega = \pm 2\omega_r$ are more sensitive to the coupling strength, as the comparison of Figs. 6(a)–6(c) demonstrates.

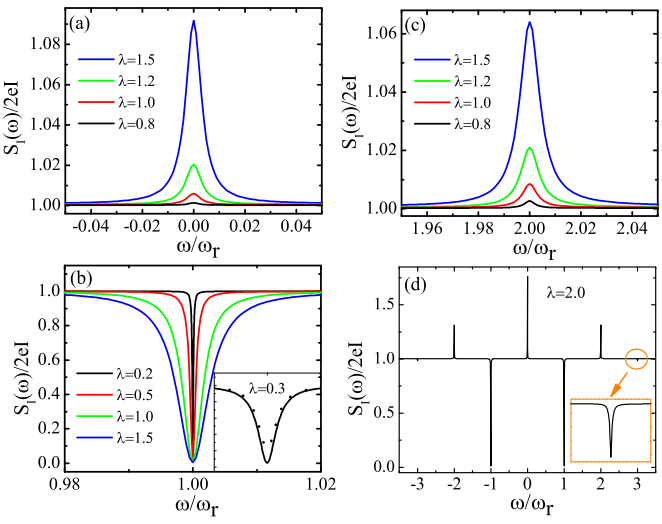

FIG. 6. (Color online) The noise spectrum of the transport current through the tunnel junction for strong coupling (a) around zero-frequency, (b) for single-photon, (c) two-photon, and (d) generally many-photon processes, respectively. The dotted line in the insets of (b) is obtained in the weak/moderate coupling approximation Eq. (20). It well describes the single-photon process in the noise spectrum for $\lambda \lesssim 0.2$. The parameters are the same as in Fig. 4.

The peaks at $\omega = 0, \pm 2\omega_r$ are always positive even at higher temperatures. Three-photon effects, which we find by expanding further, lead again to a dip in the noise spectrum at $\omega = \pm 3\omega_r$, as shown in Fig. 6(d), with properties similar to the one-photon signal. We expect that the noise spectrum in the low temperature limit shows alternating dips and peaks for odd- [at $\omega = (2n+1)\omega_r$] and even-photon-number processes (at $\omega = 2n\omega_r$, $n = 0,1,2\ldots$), respectively. This alternation of dips and peaks would be modified if also higher modes of the resonator couple to the tunnel junction. For instance, a first harmonic mode with frequency $2\omega_r$ would induce a dip resonant feature due to the single-photon processes at $\omega = 2\omega_r$, which could be larger than the second-order peak due the two-photon process with the frequency ω_r.

V. COMPARISON WITH OTHER WORK

Models similar to the one considered in this paper have been studied in other contexts with partially similar, partially differing results. For instance, tunnel junctions coupled to nanomechanical resonators were studied since they allow probing the amplitude of the position [24,26,27,29]. In that case the current noise shows a peak at $\omega = \pm\omega_r$ rather than a dip. However, one should note that in this case the oscillator couples to the height of the barrier and not to the potential difference, which we considered in our model. Another example has been studied in Ref. [28]. There the resonator was coupled to the potential difference of a metallic double dot with negligible charging energy. In this case a dip-peak feature was found. A similar dip-peak feature was obtained in Ref. [15], where a resonator coupled to a small semiconductor double dot with large charging energy has been studied. On the other hand, our results concerning single-electron tunneling through a tunnel junction coupled to a resonator are quite similar to those found when electrons tunnel through a single quantum dot coupled to a resonator, which is the case studied in Ref. [16]. Finally we mention that electron transport through quantum point contacts with an energy-dependent transmission may lead to the emission of antibunched photons [39]. These effects are not observed for the tunnel junction considered in this work. We conclude that the noise spectra in the different systems, in spite of having generally similar properties, are very sensitive to details of the coupling.

In this work we concentrated on the sequential tunneling regime, i.e., we ignored higher order correlated tunneling processes such as co-tunneling and beyond. This is for most purposes sufficient as long as the tunneling resistance is high as compared to the quantum resistance, i.e., $\eta \ll 1$. For extensions to stronger tunneling the approach described in Ref. [40] would be appropriate. In this work also the effect of a resonator bath was considered, however, concentrating on the physics of boson-assisted tunneling due to an equilibrium bath. Another approach to account for the effect of a fluctuating environment with arbitrary spectral functions is the so-called $P(E)$ description [41]. Again the majority of published work concentrates on an equilibrium bath. The major conclusion is that the tunneling system exchanges energy with the bath, which leads to a broadening of all features. As we discuss in the appendix the damping of the resonator leads to such

effects. However, for high-Q resonators considered here, the effect can be ignored.

VI. SUMMARY

In summary, we have investigated the properties of a tunnel junction coupled to a transmission line resonator. Our study is based on a Born-Markov master equation in the polaron description, which accounts for the nonequilibrium state of the resonator. We presented results for two regimes of coupling strength between resonator and tunnel junction. For weak coupling the properties are characterized by single-photon processes, for stronger coupling multiple photon processes gain importance.

For weak to moderate coupling, i.e., in the single-photon limit, we obtained analytical results at low temperatures for both the average number of the excited photons and the average current, both showing a threshold behavior when the bias voltage allows the excitation of photons. The photon distribution can be parametrized by a thermal one with an enhanced effective temperature. For the electroluminesence of the resonator we found the optimal conditions, with maximum peak height and still narrow linewidth, when the resonator damping due to the tunnel junction is comparable in strength to the intrinsic decay rate of the resonator. The current noise spectrum shows a pronounced dip at the resonator frequency.

These phenomena could be tested in experiments, since all the parameters are within reach of current technology [2,10,11,19,30,31,42].

In the strong-coupling regime, multiphoton effects can be observed. The effect of the tunnel junction on the resonator no longer reduces to an effective heating. The average number of photons excited in the resonator, which first grows with increasing coupling strength, eventually even decreases. The multiphoton effects are most pronounced in the noise spectrum of the transport current in the junction. In addition to the dips at $\omega = \pm\omega_r$ it shows peaks at $\omega = \pm 2\omega_r$, dips at $\omega = \pm 3\omega_r$, and so forth due to the interplay of the electrons tunneling through the junction associated with the emission and absorption of two photons and three photons in the resonator, respectively. The current voltage characteristic shows a threshold behavior at voltages eV which are multiples of the resonator frequency. These noise spectra are very sensitive to the details of specific system, i.e., tunnel junction versus single- or double-dot systems with either small or large charging energy, and the specific coupling mechanism between the electron transport system and the resonator. This makes the correlation functions a very useful object of theoretical and experimental studies.

ACKNOWLEDGMENTS

We acknowledge stimulating discussions with K. Ensslin, T. Ihn, A. Wallraff, X. Q. Li, Y. J. Yan, P.-Q. Jin, D. Golubev, and A. Heimes. J.S.J. acknowledges support from a fellowship of the KIT, as well as support from the Program of HNUEYT, ZNSF of China (Grant No. LZ13A040002), and the NNSF of China (Grant No. 11274085).

APPENDIX: DAMPING OF THE RESONATOR

The complete Hamiltonian of the system, including a bath with annihilation (creation) operators b_i ($b_i^\dagger$) coupling to the resonator, is given by

$$\begin{aligned} H = &\sum_{\alpha k} \varepsilon_{\alpha k} c_{\alpha k}^\dagger c_{\alpha k} + \sum_{kk'} (t_{kk'} c_{Lk}^\dagger c_{Rk'} + \text{H.c.}) \\ &+ \omega_r a^\dagger a + g \sum_k (c_{Rk}^\dagger c_{Rk} - c_{Lk}^\dagger c_{Lk})(a + a^\dagger) \\ &+ (a + a^\dagger) \sum_i g_i (b_i + b_i^\dagger) + \sum_i \omega_i b_i^\dagger b_i \,. \end{aligned} \tag{A1}$$

After a polaron transformation using the unitary operator $U = \exp[\frac{g}{\omega_r} \sum_k (c_{Rk}^\dagger c_{Rk} - c_{Lk}^\dagger c_{Lk})(a^\dagger - a)]$ we get

$$\begin{aligned} H_1 = &\sum_{\alpha k} \varepsilon_{\alpha k} c_{\alpha k}^\dagger c_{\alpha k} + \omega_r a^\dagger a \\ &+ \sum_{kk'} \left(t_{kk'} c_{Lk}^\dagger c_{Rk'} e^{-\frac{2g}{\omega_r}(a^\dagger - a)} + \text{H.c.} \right) \\ &+ (a + a^\dagger) \sum_i g_i (b_i + b_i^\dagger) + \sum_i \omega_i b_i^\dagger b_i \\ &- \frac{g}{\omega_r} \sum_k (c_{Rk}^\dagger c_{Rk} - c_{Lk}^\dagger c_{Lk}) \sum_i g_i (b_i + b_i^\dagger). \end{aligned} \tag{A2}$$

In this form we note that the bath of the resonator also couples to the potential difference between the left and right lead. In the limit $2g/\omega_r \ll 1$ we can neglect this term, and we arrive at the model analyzed in this paper. However, we also want to consider the limit $2g/\omega_r \geqslant 1$. In this case the model depends on the size and distribution of g_i. However, we will show now that the effects introduced by this coupling are small, which justifies our model in all parameter regimes.

To analyze the effect of the bath-resonator coupling term we perform another unitary transformation given by

$$U = \exp\left[-\frac{g}{\omega_r} \sum_k (c_{Rk}^\dagger c_{Rk} - c_{Lk}^\dagger c_{Lk}) \sum_i \frac{g_i}{\omega_i} (b_i^\dagger - b_i) \right]. \tag{A3}$$

This leads to the Hamiltonian,

$$\begin{aligned} H_1' = &\sum_{\alpha k} \varepsilon_{\alpha k} c_{\alpha k}^\dagger c_{\alpha k} + \omega_r a^\dagger a \\ &+ \sum_{kk'} \left(t_{kk'} c_{Lk}^\dagger c_{Rk'} e^{-\frac{2g}{\omega_r}(a^\dagger - a)} e^{-\frac{2g}{\omega_r} \sum_i \frac{g_i}{\omega_i}(b_i - b_i^\dagger)} + \text{H.c.} \right). \\ &+ (a + a^\dagger) \sum_i g_i (b_i + b_i^\dagger) + \sum_i \omega_i b_i^\dagger b_i \\ &+ g \left(\sum_i \frac{g_i^2}{\omega_r \omega_i} \right) \sum_k (c_{Rk}^\dagger c_{Rk} - c_{Lk}^\dagger c_{Lk})(a + a^\dagger). \end{aligned} \tag{A4}$$

Repeating the procedure shown here one more time we get

$$H_2' = \sum_{\alpha k} \varepsilon_{\alpha k} c_{\alpha k}^\dagger c_{\alpha k} + \omega_r a^\dagger a + \sum_{kk'} \left(t_{kk'} c_{Lk}^\dagger c_{Rk'} e^{-\frac{2g}{\omega_r}(1+x)(a^\dagger - a)} e^{-\frac{2g}{\omega_r}(1+x)\sum_i \frac{g_i}{\omega_i}(b_i - b_i^\dagger)} + \text{H.c.} \right)$$
$$+ (a + a^\dagger) \sum_i g_i (b_i + b_i^\dagger) + \sum_i \omega_i b_i^\dagger b_i + g x^2 \sum_k (c_{Rk}^\dagger c_{Rk} - c_{Lk}^\dagger c_{Lk})(a + a^\dagger), \tag{A5}$$

with $x = \sum_i g_i^2/(\omega_r \omega_i)$. We did not specify the precise form of the spectral function of the bath of the resonator. However, since the coupling between resonator and bath is weak we can safely assume $x < 1$. In this case we can repeat this procedure to all orders and get

$$H_\infty' = \sum_{\alpha k} \varepsilon_{\alpha k} c_{\alpha k}^\dagger c_{\alpha k} + \omega_r a^\dagger a + \sum_{kk'} \left(t_{kk'} c_{Lk}^\dagger c_{Rk'} e^{-\frac{2g}{\omega_r(1-x)}(a^\dagger - a)} e^{-\frac{2g}{\omega_r(1-x)}\sum_i \frac{g_i}{\omega_i}(b_i - b_i^\dagger)} + \text{H.c.} \right)$$
$$+ (a + a^\dagger) \sum_i g_i (b_i + b_i^\dagger) + \sum_i \omega_i b_i^\dagger b_i. \tag{A6}$$

In this form we note that in comparison to the model Hamiltonian (2) we produced a renormalization of the coupling constant between the tunneling term and the resonator, $g \to g/(1-x)$, and in addition a coupling between the tunneling term and the reservoir of the resonator $\exp[-\frac{2g}{\omega_r(1-x)}\sum_i \frac{g_i}{\omega_i}(b_i - b_i^\dagger)]$. The latter is well known in quantum transport under the name $P(E)$ theory [41]. It leads to a broadening of the energy dependence of the rates and all other features discussed in this paper. However, the effect is small as long as the resonator has a high Q factor.

[1] A. Blais, R.-S. Huang, A. Wallraff, S. M. Girvin, and R. J. Schoelkopf, Phys. Rev. A **69**, 062320 (2004).

[2] A. Wallraff, D. I. Schuster, A. Blais, L. Frunzio, J. M. R. S. Huang, S. Kumar, S. M. Girvin, and R. J. Schoelkopf, Nature (London) **431**, 162 (2004).

[3] I. Chiorescu, P. Bertet, K. Semba, Y. Nakamura, C. J. P. M. Harmans, and J. E. Mooij, Nature (London) **431**, 159 (2004).

[4] J. Majer, J. M. Chow, J. M. Gambetta, J. Koch, B. R. Johnson, J. A. Schreier, L. Frunzio, D. I. Schuster, A. A. Houck, A. Wallraff *et al.*, Nature (London) **449**, 443 (2007).

[5] M. A. Sillanpää, J. I. Park, and R. W. Simmonds, Nature (London) **449**, 438 (2007).

[6] M. Hofheinz, H. Wang, M. Ansmann, R. C. Bialczak, E. Lucero, M. Neeley, A. D. O'Connell, D. Sank, J. Wenner, J. M. Martinis *et al.*, Nature (London) **459**, 546 (2009).

[7] O. Astafiev, K. Inomata, A. O. Niskanen, T. Yamamoto, Y. A. Pashkin, Y. Nakamura, and J. S. Tsai, Nature (London) **449**, 588 (2007).

[8] J. Hauss, A. Fedorov, C. Hutter, A. Shnirman, and G. Schön, Phys. Rev. Lett. **100**, 037003 (2008).

[9] M. Grajcar, S. H. W. van der Ploeg, A. Izmalkov, H. G. M. E. Ilichev, A. Fedorov, A. Shnirman, and G. Schön, Nat. Phys. **4**, 612 (2008).

[10] T. Frey, P. J. Leek, M. Beck, K. Ensslin, A. Wallraff, and T. Ihn, Appl. Phys. Lett. **98**, 262105 (2011).

[11] T. Frey, P. J. Leek, M. Beck, A. Blais, T. Ihn, K. Ensslin, and A. Wallraff, Phys. Rev. Lett. **108**, 046807 (2012).

[12] M. R. Delbecq, V. Schmitt, F. D. Parmentier, N. Roch, J. J. Viennot, G. Fève, B. Huard, C. Mora, A. Cottet, and T. Kontos, Phys. Rev. Lett. **107**, 256804 (2011).

[13] L. Childress, A. S. Sørensen, and M. D. Lukin, Phys. Rev. A **69**, 042302 (2004).

[14] P.-Q. Jin, M. Marthaler, J. H. Cole, A. Shnirman, and G. Schön, Phys. Rev. B **84**, 035322 (2011).

[15] J. Jin, M. Marthaler, P.-Q. Jin, D. Golubev, and G. Schön, New J. Phys. **15**, 025044 (2013).

[16] C. Bergenfeldt and P. Samuelsson, Phys. Rev. B **85**, 045446 (2012).

[17] M. Schiro and Karyn Le Hur, Phys. Rev. B **89**, 195127 (2014).

[18] J. R. Souquet, I. Safi, and P. Simon, Phys. Rev. B **88**, 205419 (2013).

[19] C. Altimiras, O. Parlavecchio, P. Joyez, D. Vion, P. Roche, D. Esteve, and F. Portier, Phys. Rev. Lett. **112**, 236803 (2014).

[20] S. A. Gurvitz, Phys. Rev. B **56**, 15215 (1997).

[21] A. N. Korotkov, Phys. Rev. B **63**, 115403 (2001).

[22] J. M. Elzerman, R. Hanson, L. H. Willems van Beveren, B. Witkamp, L. M. K. Vandersypen, and L. P. Kouwenhoven, Nature (London) **430**, 431 (2004).

[23] T. Fujisawa, T. Hayashi, R. Tomita, and Y. Hirayama, Science **312**, 1634 (2006).

[24] M. Poggio, M. P. Jura, C. L. Degen, M. A. Topinka, H. J. Mamin, D. Goldhaber-Gordon, and D. Rugar, Nat. Phys. **4**, 635 (2008).

[25] J. Stettenheim, M. Thalakulam, F. Pan, M. Bal, Z. Ji, W. Xue, L. Pfeiffer, K. W. West, M. P. Blencowe, and A. J. Rimberg, Nat. Lett. **466**, 86 (2010).

[26] A. A. Clerk and S. M. Girvin, Phys. Rev. B **70**, 121303 (2004).

[27] S. Walter and B. Trauzettel, Phys. Rev. B **83**, 155411 (2011).

[28] L. L. Benatov and M. P. Blencowe, Phys. Rev. B **86**, 075313 (2012).

[29] D. Mozyrsky and I. Martin, Phys. Rev. Lett. **89**, 018301 (2002).

[30] G. Gasse, C. Lupien, and B. Reulet, Phys. Rev. Lett. **111**, 136601 (2013).

[31] J.-C. Forgues, C. Lupien, and B. Reulet, Phys. Rev. Lett. **113**, 043602 (2014).

[32] S. André, P. Q. Jin, V. Brosco, J. H. Cole, A. Romito, A. Shnirman, and G. Schön, Phys. Rev. A **82**, 053802 (2010).

[33] M. Scully and M. S. Zubairy, *Quantum Optics* (Cambridge University Press, Cambridge, 1997).

[34] X. Q. Li, J. Y. Luo, Y. G. Yang, P. Cui, and Y. J. Yan, Phys. Rev. B **71**, 205304 (2005).

[35] U. Gavish, Y. Levinson, and Y. Imry, Phys. Rev. B **62**, R10637(R) (2000).

[36] H. J. Carmichael, *An Open System Approach to Quantum Optics* (Spring-Verlag, Berlin, 1993).

[37] R. Loudon, *The Quantum Theory of Light*, 2nd ed. (Clarendon Press, Oxford, 1983).

[38] H. P. Breuer and F. Petruccione, *The Theory of Open Quantum Systems* (Oxford University Press, Oxford, 2002).

[39] C. W. J. Beenakker and H. Schomerus, Phys. Rev. Lett. **86**, 700 (2001); **93**, 096801 (2004).

[40] J. König, J. Schmid, H. Schoeller, and G. Schön, Phys. Rev. B **54**, 16820 (1996).

[41] See, for instance, G.-L. Ingold and Yu. V. Nazarov, in *Single Charge Tunneling*, edited by H. Grabert and M. H. Devoret, NATO ASI Series B (Plenum Press, New York, 1992), Vol. 294, pp. 21–107.

[42] N. Ubbelohde, C. Fricke, C. Flindt, F. Hohls, and R. J. Haug, Nat. Commun. **3**, 612 (2012).